

Space-Based Global Maritime Surveillance. Part II: Artificial Intelligence and Data Fusion Techniques

Giovanni Soldi , **Domenico Gaglione** , and **Nicola Forti** , NATO Centre for Maritime Research and Experimentation (CMRE), 19126 La Spezia, Italy
Alessio Di Simone , University of Naples Federico II, 80125 Naples, Italy
Filippo Cristian Daffinà, E-GEOS, 00156, Rome, Italy
Gianfausto Bottini, FAO, 00153, Rome, Italy
Dino Quattrociocchi, e-GEOS, Rome, 00156, Italy
Leonardo M. Millefiori , **Paolo Braca** , and **Sandro Carniel**, NATO Centre for Maritime Research and Experimentation (CMRE), 19126 La Spezia, Italy
Peter Willett , University of Connecticut, Storrs, CT 06269 USA
Antonio Iodice and Daniele Riccio , University of Naples Federico II, 80125 Naples, Italy
Alfonso Farina , Consultant, 00144 Rome, Italy

AIS和星载检测的融合

INTRODUCTION

Maritime surveillance (MS) aims at providing seamless wide-area operational pictures in coastal areas and the oceans in real time. Multiple heterogeneous sensors and information sources are nowadays available for MS, all with their advantages and limitations, and significant research and engineering effort has been made for their combination. Besides the most common terrestrial sensors for MS, e.g., the automatic identification system (AIS), X-band radars, and over-the-horizon (OTH) radars, space-based sensor technologies enable persistent monitoring of the maritime domain and ship traffic on a global scale even in remote areas of the Earth. Space-based remote sensing technologies, reviewed in the first part of this work [1], include satellite-based AIS (Sat-AIS), synthetic

aperture radar (SAR), multispectral (MSP) and hyperspectral (HSP) optical sensors, and global navigation satellite systems reflectometry (GNSS-R). Space-based sensors for Earth observation allow collecting images of very large areas in remote regions of the globe with relatively short latency and, hence, are strongly relevant to MS.

As a consequence of the deployment and spread of space-based sensor technologies, advanced data processing paradigms, e.g., big data analysis, machine learning, artificial intelligence (AI), and data fusion, are now extremely needed to fully exploit the wide availability of large datasets of satellite images. In particular, the development of MS systems combining multiple sensors requires dedicated algorithms to process raw satellite images, detect and classify ships, and fuse information from heterogeneous sensors. These algorithms support MS by processing and organizing the increasing amount of heterogeneous information. The extracted data and readily understandable information digested therefrom will help end-users, such as governmental and military authorities, coast guards, and police, to detect anomalies, threats such as oil spills, piracy, and human trafficking, and act in time to prevent accidents and wrongdoing. In this second part of our work, we describe some recent AI and image processing techniques for image segmentation, target detection, and classification, and provide possible use cases with real images acquired by satellite sensors. Then, we describe recent Bayesian and statistical fusion techniques to extract knowledge from the troves of historical Sat-AIS data, such as most common maritime routes, and to track multiple targets by fusing information collected by multiple heterogeneous sensors. Among these, multitarget tracking (MTT) algorithms based on the sum-product algorithm (SPA) are gaining popularity, thanks to their ability to fuse information

Authors' current addresses: G. Soldi, D. Gaglione, N. Forti, L. M. Millefiori, P. Braca, S. Carniel, NATO Centre for Maritime Research and Experimentation (CMRE), 19126 La Spezia, Italy (e-mail: giovanni.soldi@cmre.nato.int). A. Di Simone, A. Iodice, D. Riccio, University of Naples Federico II, 80125 Naples, Italy. F. C. Daffinà, D. Quattrociocchi, e-GEOS, 00156 Rome, Italy. G. Bottini, FAO, 00153 Rome, Italy. P. Willett, Department of Electrical and Computer Engineering, University of Connecticut, Storrs, CT 06269 USA. Alfonso Farina, Consultant, 00144 Rome, Italy.

Manuscript received November 7, 2020, revised January 20, 2021; accepted February 25, 2021, and ready for publication April 1, 2021.

Review handled by Maria Sabrina Greco.

0885-8985/21/\$26.00 © 2021 IEEE



Credit: Image licensed by Ingram Publishing

from heterogeneous sources, to their scalability, i.e., low computational complexity in terms of the numbers of information sources, targets, and measurements, and to their capability to include contextual information, e.g., maritime routes and ships class information extracted from satellite images. A use case that confirms the strength of SPA-based MTT algorithms when combined with information acquired by satellite sensors is also provided.

ADVANCED AI TECHNIQUES FOR SATELLITE SENSOR DATA

The proliferation of space-based sensors collecting images of the Earth has called for the development of advanced AI and imaging techniques to extract ship features and identities to improve the surveillance capability. In particular, and analogous to many other scientific fields, deep neural network (DNN) techniques for detection and segmentation of specific targets from satellite images have recently received increasing interest. Advanced AI and DNN techniques allow, for example, the production of a “digital report” for any satellite image by performing vessel detection, segmentation, classification, and identification, by estimating ships dimensions and headings, and by providing geographic coordinates and timestamps. Figure 1 shows two examples of satellite images augmented by a digital report for each detected ship.

In this section, we provide a review of some AI and statistical techniques for object detection, segmentation, and classification in satellite images that are used in our study.

DNN ARCHITECTURES FOR SATELLITE IMAGE SEGMENTATION AND TARGET CLASSIFICATION

Complex DNNs with multiple hidden layers and neurons can be used for satellite image segmentation and target classification. The training of these DNNs requires large labeled

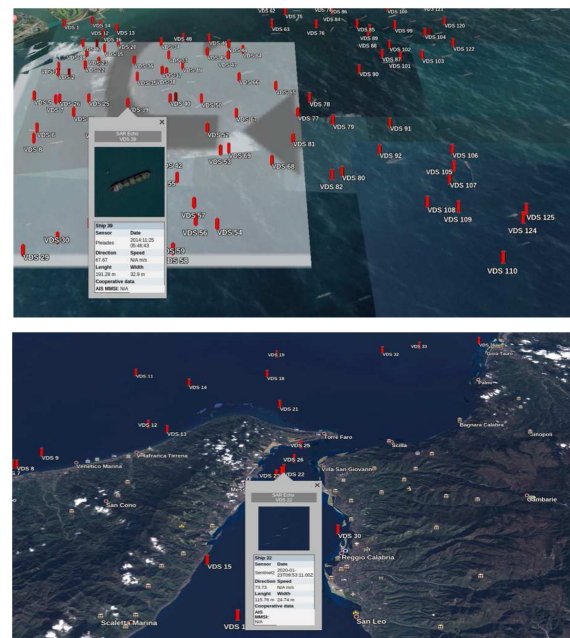
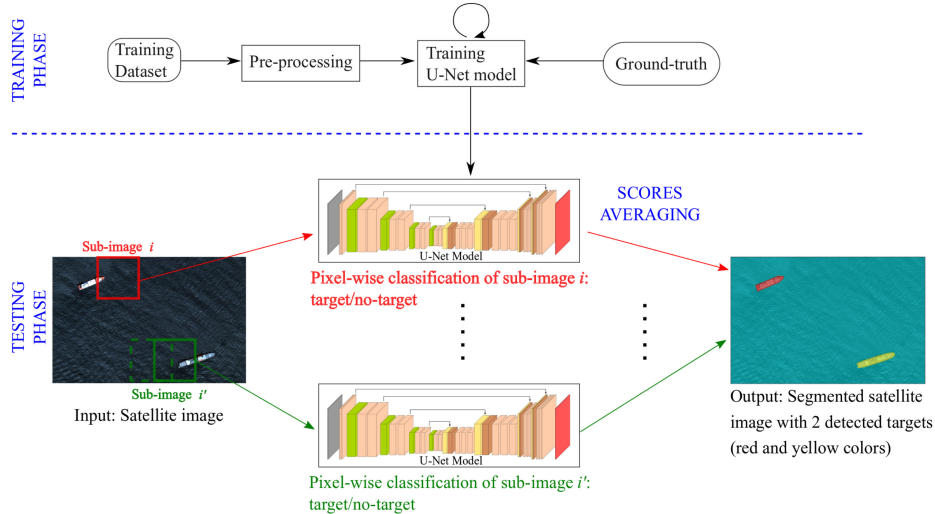


Figure 1.

Examples of satellite images augmented by a digital report for each detected ship. (Top) MSP sensor: Pleiades, Area: close to Khark island (Iran), Date: 25th November 2014. (Bottom) MSP sensor: Sentinel-2, Area: Strait of Messina (Italy), Date: 23rd January 2020.

**Figure 2.**

General workflow example of a satellite image segmentation task based on the U-Net architecture, where pooling operations are replaced by upsampling operators. The chosen DNN architecture is trained to perform pixelwise classification (target/no-target) using a training dataset of preprocessed satellite images that have been segmented manually in accordance with the ground-truth (training phase). During this phase, the U-Net model parameters are optimized by minimizing an appropriate cost function. The trained U-Net model is then used to perform pixelwise classification on a test satellite image (testing phase). Concretely, a test satellite image is divided into N subimages; for each subimage i , the final Softmax layer in the U-Net model assigns a classification score to each pixel. The segmented satellite image is eventually obtained by averaging the scores assigned to each pixel in the overlapping subimages.

datasets, and this is naturally demanding both of storage and of computational power. Graphical processing units (GPUs) are the key to address the computational demand. Data augmentation techniques, such as cropping, padding, and flipping, enable practitioners to significantly increase the diversity of data images available to train large DNN models, without actually collecting new images. For image segmentation and target classification, convolutional neural network (CNN) architectures are the most common, since they allow for an efficient analysis of image textures, i.e., the contextual signal from the neighboring pixels of a pixel under test. During the training phase of a CNN, features automatically extracted from a set of training images are assessed to understand (learn) which of them are the most suitable and relevant to perform segmentation and/or classification. Some common CNN architectures used for image segmentation and classification are the U-Net [2], the residual CNNs, e.g., ResNet [3], and the mask region-based CNN (R-CNN) [4]. The U-Net is mostly used for pixelwise classification; ResNet is mainly used for target or object classification tasks; and the Mask R-CNN, instead, is a region-based CNN mostly used to perform image segmentation by providing as output bounding boxes around identified targets. Figure 2 depicts a general workflow example of a satellite image segmentation task based on the U-Net architecture.

USE CASES: AI TECHNIQUES FOR SATELLITE IMAGE SEGMENTATION AND CLASSIFICATION

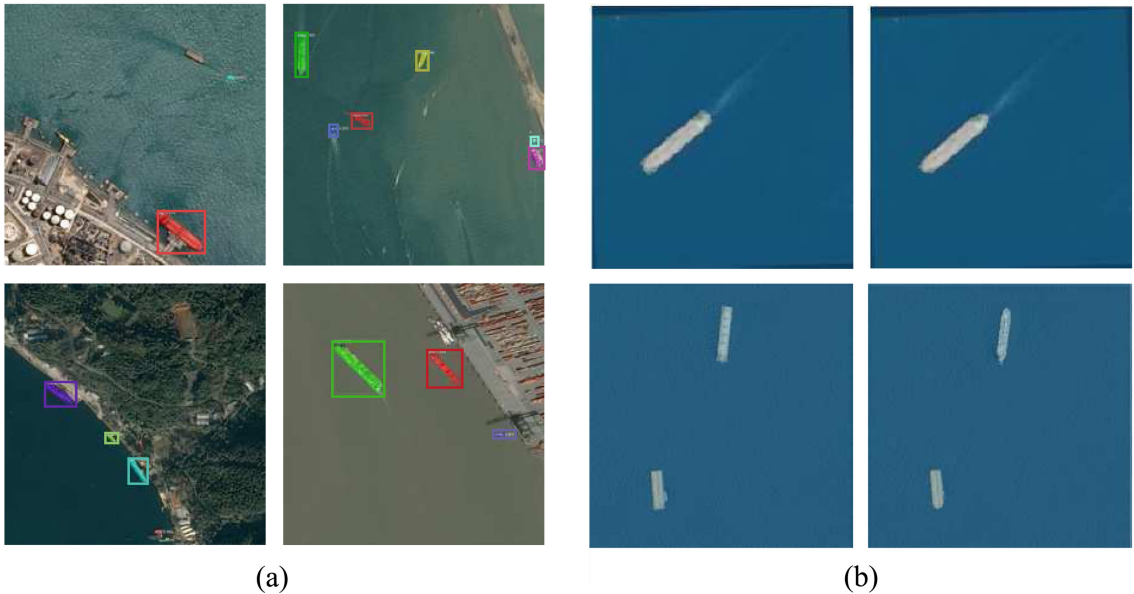
The first use case that we present is to detect ships and extract important features, e.g., position, width, length,

heading, and other relevant information, from very high-resolution (VHR) optical satellite images by means of CNNs. The training dataset consists of about 200 thousand VHR images, with spatial resolution of approximately 1.5 m and dimension 768 by 768 pixels, acquired by the GeoEye, SPOT, Pleiades, and Black Sky satellites. The inference, i.e., the testing of the CNN, is performed on new images acquired by the same sensors. A Mask R-CNN architecture is used, and Figure 3(a) shows an example result of the segmentation task: detected ships are surrounded by bounding boxes and highlighted with different colors.

The second use case is the segmentation of high-resolution (HR) images, with spatial resolution of about 10 m. A synthetic dataset of HR images is obtained by degrading 10 thousand VHR images acquired by SPOT satellite, by means of appropriate computer vision techniques, such as the pyramid representation [5], in which an image is subject to repeated smoothing and subsampling. The type of architecture employed in this case is the U-Net, and Figure 3(b) represents an example result of the segmentation task, which ran over a validation dataset of HR images. In particular, the left-hand side images of Figure 3(b) represent the ground-truth, i.e., ships are manually extracted, while the right-hand side images represents the output of the segmentation task.

The third use case is related to the classification between ship stern and bow by means of a ResNet34 architecture. The training dataset is composed of satellite images acquired by Sentinel-2 (S-2), from which detected ships are clipped, manually divided into stern and bow, and labeled. Figure 4 represents the results of the classification.

In order to have a more complete view of the maritime situational picture, DNNs can be also conceived to

**Figure 3.**

(a) Example result of the segmentation task on VHR images (first use case): detected ships are surrounded by bounding boxes and highlighted with different colors. (b) Example result of the segmentation task ran over a validation dataset of HR images (second use case): left-hand side images represent the ground-truth, i.e., ships are manually extracted, while the right-hand side images represent the output of the segmentation task.

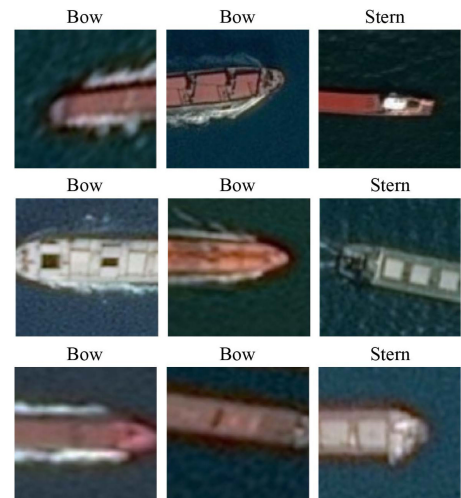
discriminate among different types of vessels, by exploiting the heterogeneous information contained in historical Sat-AIS messages. In particular, the information provided by historical Sat-AIS data, e.g., ship width, length, and type, can be used to train neural networks to classify vessels into 14 categories derived by the AIS ship type, i.e., antipollution-law, medical-nonconflict, cargo, dredging-military-sailboat, fishing, high-speed craft, other-unknown-reserved, passenger, pilot boat, pleasure, search and rescue, tanker, tug-towing, wing in ground-effect. The neural network architecture used to perform this classification task consists of 2 hidden layers, the first with 200 neurons and the second with 100 neurons, and of an output layer of 14 neurons, with each neuron providing the probability of belonging to the respective category. During the inference phase, the neural network utilizes the information, e.g., length, width, and area, provided by a segmentation task on VHR or HR satellite images, to categorize each of the detected vessels into one of the 14 classes.

EXTRACTING KNOWLEDGE FROM SAT-AIS DATA

Sat-AIS is a common technology to obtain a comprehensive and global picture of maritime traffic, including that of areas far from ports and shore. AIS messages can be collected by low Earth orbit satellite systems and provide a global capability for maritime traffic monitoring using constellations of satellites and a network of globally distributed ground-based stations. This offers several benefits, including enhanced monitoring of fine-scale vessel behavior and traffic patterns, improved ability to identify potential threats, and more

cost-effective use of assets. The global coverage enabled by space-based technology is a key feature that led Sat-AIS to become the major source, by volume and coverage, of maritime traffic information for global-scale monitoring. Nowadays, AIS data have been of an increasing value, not only for ships themselves, but especially for coast guards, naval forces, and other marine operational authorities that can exploit such data to improve MS.

The availability of global datasets provided by Sat-AIS technology opens up new ways to extract valuable

**Figure 4.**

Stern and bow classification for detected ships in clipped satellite images acquired by S-2.

knowledge for MS. However, with the increase of the available Sat-AIS data to massive scales, computational strategies must cope with challenges typically faced when collecting, storing, querying, and processing globally distributed datasets of considerable size. Vast amounts of data tend to overwhelm human operators and call for approaches with a high degree of automation. Furthermore, standard algorithms are proving to be unable to deal with the nonidealities (e.g., erroneous, incomplete, intermittent, or counterfeit information) of such datasets. As an example, in contrast with traditional positional measurements, Sat-AIS messages are irregularly sampled, with an update interval usually dependent on the specific vessel's kinematic behavior. Moreover, ships can enter and exit the receivers' network coverage; or, worse, intentionally disable Sat-AIS transmitters. All this can lead to surveillance gaps that range from several minutes to many hours. From this perspective, the success of future surveillance systems using maritime data will increasingly require to combine statistical, big data analytics, and AI techniques in order to handle all the aforementioned challenges introduced by AIS datasets.

AIS-BASED MARITIME TRAFFIC KNOWLEDGE DISCOVERY

An important task to further improve MS is capitalizing on the ever growing trove of available AIS data by turning this information into actionable knowledge of the maritime situational picture at a global scale. During the last two decades, a significant body of research has been dedicated to the development of new methodologies, as well as commercial products, e.g., the multiple intelligence analytics for pattern learning and exploitation (MAPLE) developed by BAE Systems, in support of MS. They aim at learning, from historical AIS data and, if available, other information sources (e.g., SAR images), motion patterns of ships [6]–[12] (i.e., recurrent sea routes and statistical analytics about the dynamics), and density and types of vessels [13] that, if well-characterized, can be beneficial for different MS applications such as anomaly detection [14], [15], knowledge-based tracking [16], classification, and long-term prediction of vessels [17].

Knowledge discovery of maritime traffic patterns from AIS data can be broadly classified [18], [19] into statistics-, grid-, and vector-based methods. In addition, machine learning tools have been explored to encode AIS historical (training) data for vessel trajectory prediction [20]–[22]. Statistics-based techniques [23], [24] focus on analyzing the available data in order to provide a visual representation and quantitative modeling of the fundamental statistical analytics. Grid-based methods [6]–[8], [10] divide the area of interest into a spatial grid of indexed cells, each dealing with the static and dynamic properties of those vessels that passed through the specific element of the grid. This presents the benefit of reducing the overall scale of the information extraction

process, as well as the storage for fast query/search operations. Finally, vector-based methods [9] use a chain representation of maritime traffic, considering sea routes as a set of links connecting waypoints. This allows for high compactness of the waypoints and traffic routes representation at a global scale. A vector-based approach leveraging point clustering is the traffic route extraction for anomaly detection (TREAD) algorithm developed in the paper by Pallotta *et al.* [9]. TREAD generates a set of historical patterns of life represented by waypoints and route features, where waypoints are defined as stationary objects like ports and offshore platforms or entry/exit points.

Further advancements on vector-based knowledge discovery [11], [12] have recently led to the development of an unsupervised graph-based methodology to identify the spatiotemporal dynamics of ship routes, and efficiently extract a compact representation of global maritime patterns from large volumes of historical AIS data, in the form of a maritime traffic graph (MTG). This method builds on recent advances in long-term vessel motion modeling [17], [25] whereby the dynamics of ships can be effectively described by a piecewise Ornstein–Uhlenbeck (OU) mean-reverting stochastic process. This approach, extensively validated against real-world datasets [17], [26], relies on model parameters that change only at waypoints (places where ships regularly stop or change their velocity). The OU model makes it possible to statistically represent with increased accuracy the dynamics of maritime traffic, reliably predict the future positions of vessels over a long time horizon (e.g., in the order of hours), while maintaining a lower uncertainty, and reliably associate sparse (in space and time) measurements to tracks; hence, it enables the synthesis of historical ship trajectories into a sequence of waypoints connected together by a network of navigational legs (with nonmaneuvering motion between waypoints). Examples of MTGs extracted from AIS data obtained in the North sea and in the Mediterranean sea are shown in Figure 5. The MTG method works in an unsupervised way, is computationally efficient, and can deal with big data processing models and paradigms. The effectiveness of this methodology has been successfully demonstrated on real-world extensive AIS datasets collected in the Iberian Coast and English Channel areas [11], as well as during the validation phase in four operational trials of the EU-H2020 project for maritime integrated surveillance awareness (MARISA) [12]. Starting from raw AIS streams, the MTG model can be automatically extracted based on the following key data processing steps as also shown in Figure 6.

DETECTION OF NAVIGATIONAL WAYPOINTS

Based on the OU dynamic model (DM) for accurate long-term ship prediction, change detection algorithms can be applied to identify specific geospatial waypoints where the mean long-term velocity parameter of the underlying OU process tends to change [11], [27]. The detected

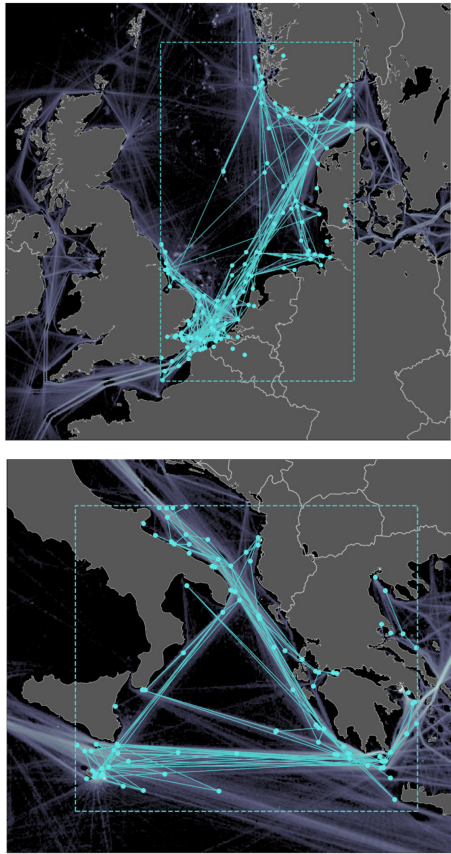


Figure 5.

MTGs extracted from AIS data obtained in the North sea (upper figure) and in the Mediterranean sea (lower figure).

waypoints represent: i) ports, where a ship's speed is null either before (leaving the port) or after the change (entering the port); ii) navigational waypoints, where the direction of the ship changes (while the speed is possibly constant); and iii) entry, exit, and entry/exit points, i.e., virtual boundary regions of the area of interest that summarize the entering and exiting traffic. In Figure 6-(top-right map), a total of 162,662 waypoints are identified during this step.

CLUSTERING OF NAVIGATIONAL WAYPOINTS

Based on the assumption that most maritime traffic is inherently regular, change points are expected to be concentrated around specific geospatial regions. To find these significant waypoint areas, standard density-based clustering techniques, such as density-based spatial clustering of applications with noise (DBSCAN) [28], can be used in order to group together multiple change points into a lower number of distinct waypoint clusters. Intuitively, a clustering algorithm will look for regions where navigational change points are very close in the feature space and will identify outliers as points lying in low-density regions. In Figure 6-(bottom-right map), a total of 2,286

clusters are found during this step (each cluster is identified by a color).

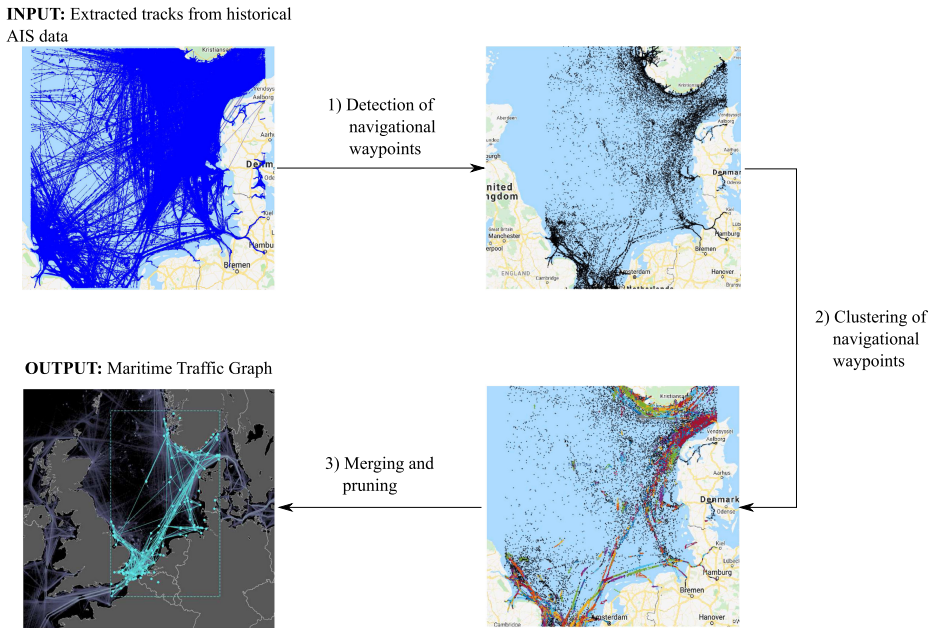
MERGING AND PRUNING PROCEDURES

When clustering algorithms are applied to large-scale real-world datasets involving a huge number of data points, the output generated by such unsupervised classification will usually need some postprocessing. To this end, pruning and merging techniques can be used to progressively improve and simplify the overall MTG by reducing the number of graph entities (i.e., nodes and edges), and thus, implicitly encode knowledge about ships' patterns using a lower-dimensional representation. The number of graph edges can be reduced by eliminating those links characterized by low weights, these being least likely to represent recurrent patterns; and by merging closely spaced edges (connecting waypoints in a cluster with waypoints in a different cluster) into one, as these are more efficiently represented by a single route. Figure 6-(bottom-left image) represents the resulting MTG, which consists of 99 nodes and 401 edges.

As a result, the structure of maritime traffic in the area of interest during a reference time interval can be represented, using graph formalism, by a directed graph $\mathcal{G} = (\mathcal{N}, \mathcal{E})$, where $\mathcal{N} = \{1, 2, \dots, N\}$ is the set of nodes, and $\mathcal{E} \subseteq \mathcal{N} \times \mathcal{N}$ is the set of edges. In particular, it is supposed that (i, j) belongs to \mathcal{E} if and only if there are ship tracks with two consecutive waypoints i and j , where node i is the predecessor of node j . In this way, the adjacency matrix of the graph \mathcal{A} can be directly constructed from the raw ship tracks data (i.e., time-ordered lists of AIS messages) by simply identifying the transitions (and associated direction) of ships from a generic pair of nodes. We naturally assume that $(i, i) \notin \mathcal{E}$ for any $i \in \mathcal{N}$, so that diagonal elements of \mathcal{A} are set to zero, i.e., \mathcal{G} is a directed simple graph with no self-loops. A graph of order (i.e., number of nodes) $|\mathcal{N}| = N$ and size (i.e., number of edges) $|\mathcal{E}| = L$ is denoted as $\mathcal{G}(N, L)$. In conclusion, the extracted waypoints and navigational legs—nodes and edges of the MTG—can be represented as vector features with different attributes directly extrapolated from the available AIS messages or computed during the graph extraction phase. The attributes of each graph entity will include aggregate georeferenced data and statistical analytics about the identified maritime patterns. The resulting geospatial information layer, that can be directly used for efficient mapping, query, and search operations, serves as a baseline reference of maritime traffic for different MS applications.

MARITIME ANOMALY DETECTION

Contextual information about historical maritime traffic extracted through knowledge discovery methods discussed

**Figure 6.**

General workflow for the extraction of a MTG model. Tracks initially extracted from historical AIS data are used as input (top-left map: 19,009 AIS tracks). In the first step, waypoints for each AIS track are identified by a statistical procedure for change detection based on the OU dynamic model (top-right map: 162,662 detected waypoints). In the second step, the identified waypoints are then clustered to identify specific geospatial regions where waypoints are concentrated (bottom-right map: 2,286 clusters with each cluster identified by a color). During the final step pruning and merging techniques can be used to encode ships' patterns in a lower-dimensional graph representation (bottom-left map: 99 nodes and 401 edges).

in the section “AIS-Based Maritime Traffic Knowledge Discovery” can be highly beneficial as prior information on the nominal dynamic behavior of vessels to determine when anomalous activities are happening. Common threats in the maritime domain include drug smuggling, piracy and terrorism, illegal immigration, marine pollution, prohibited imports/exports, or illegal, unreported, and unregulated (IUU) fishing. For decades, anomaly detection strategies have been explored and applied in maritime traffic monitoring [8], [14], [15], [29]–[33] in order to detect unexpected ship stops or unexpected changes in course, i.e., any vessel’s anomalous deviation from the standard route that might be related to an activity that requires closer attention. Most research on maritime anomaly detection [8], [29]–[31] relies on two steps: i) knowledge discovery of maritime traffic patterns from historical data, and ii) anomaly detection via unsupervised learning.

More recently, an innovative statistical framework[32], [33] that combines the available context data with a parametric model of the vessel’s kinematic behavior has received special attention. Unlike other works [8], [29]–[31], here the formulation of maritime anomaly detection is based on the OU DM [17]. While it is useful that the OU model represents targets’ motion in terms of speed and direction, its key strength is its greatly reduced prediction uncertainties: deviations from prediction are less easily explained as random noise than they would be if other models were used. This line of research has focused on the development of anomaly detection strategies that provide the ability to reveal vessel

deviations from standard navigational routes as well as *dark* deviations in the presence of possibly intentional surveillance gaps (due to AIS disablments or limited sensor coverage). Using the OU model to represent the vessel dynamics and contextual information to define the nominal behavior at the sea, the anomaly detector in [32] and [33] runs a hypothesis testing procedure—the generalized likelihood ratio test—to make decisions on the existence of anomalous deviations within a given time window relying upon the available measurements (e.g., AIS, radar, SAR). This anomaly detection method, based on the OU model and successfully applied to a real-world rendezvous detection scenario in [33], can integrate measurements from multiple sources and handle different levels of data unavailability. The use of multiple heterogeneous measurements associated with the vessel under track, e.g., AIS messages combined with noncooperative contacts from coastal surveillance radar networks or satellite networks, can lead to a significant improvement of detection performance. An additional feature of this method is the option to choose a fixed detection false alarm rate, which is a well-known issue for maritime command and control systems. Such an automatic detector enables quick reaction of human operators to anomalies at the sea with much improved chances of a productive operation for surveillance and intercept units.

Further developments [34]–[36] focused on the problem of dynamic detection of motion anomalies and joint tracking for real-time MS. Based on recent advances on hybrid Bernoulli filtering [37], which combines standard

tracking methods with optimal joint input-and-state estimation theory, a unified Bayesian framework [34], [36] has been developed for addressing the problem of sequential anomaly detection in practical surveillance applications characterized by highly cluttered environments, missed detections, and sensor data gaps. An adaptive version [35] of this Bayesian framework is capable of also handling unknown parameters in the underlying OU vessel dynamics.

BAYESIAN INFORMATION FUSION AND MTT FOR MS

The main purpose of a multisensor MTT algorithm is to sequentially determine the number of ships in the MS area and estimate their states, e.g., position, velocity, course, and heading, by exploiting measurements from multiple heterogeneous sensors. The measurements are noisy observations of the kinematics, dimensions, shapes, or other features of the targets that can also be output of a classifier. The MTT problem, thus, consists of a detection step and an estimation step; mathematically, these can be formalized as follows. We denote with $x_{n,1}, \dots, x_{n,K_n}$ the unknown states of K_n targets at time n , with $z_{n,1}^{(s)}, \dots, z_{n,M_n^{(s)}}^{(s)}$ the $M_n^{(s)}$ measurements generated by sensor s at time n , and with z all the measurements from all sensors up to time n . Figure 7 represents examples of measurements $z_{n,m}^{(s)}$ that could be extracted from a MSP image acquired by a S-2 optical sensor by means of a segmentation and classification technique, as described in the section “DNN Architectures for Satellite Image Segmentation and Target Classification.” Based on the measurements z , the likelihood functions $f(z_{n,m}^{(s)}|x_{n,k})$, and the probability density functions (pdfs) $f(x_{n,k}|x_{n-1,k})$, which model an appropriate DM, e.g., the OU DM, we wish to

- 1) (*Detection step*) estimate the number of targets \hat{K}_n ;
- 2) (*Estimation step*) estimate the target states $\hat{x}_{n,1}, \dots, \hat{x}_{n,\hat{K}_n}$.

In a Bayesian formulation, the estimation step essentially amounts to calculating at each time n , the posterior pdfs $f(x_{n,k}|z)$ of the states $x_{n,k}$ given all the measurements up to current time z . MTT methods have to cope with various challenges, for example, the heterogeneity of the different information sources [38]–[40], and the measurement-origin uncertainty (MOU), i.e., the fact that it is unknown which target (if any) generated which measurement.

Existing MTT algorithms can be broadly classified as “vector-type” algorithms, such as the joint probabilistic data association (JPDA) filter [41] and the multiple hypothesis tracker (MHT) [42], [43], and “set-type” algorithms, such as the (cardinalized) probability hypothesis density filter [44]–[47], and multi-Bernoulli filters [44], [48]. Vector-type algorithms represent the multitarget states and measurements by random vectors, whereas set-type algorithms represent them by random finite sets.

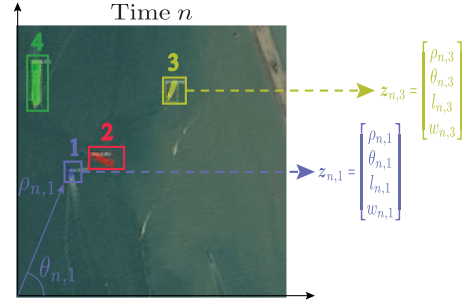


Figure 7.

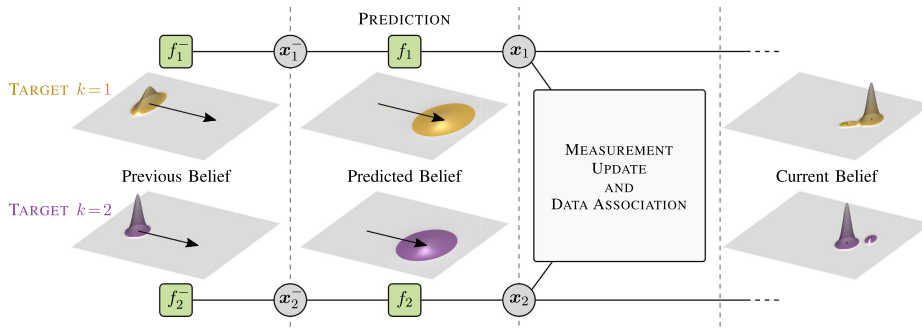
Example of measurements $z_{n,m}$ (sensor index s is omitted for clarity) extracted at time n from four detected ships in a MSP image acquired by S-2 satellite. In this example scenario, each measurement $z_{n,m}$ consists of range $\rho_{n,m}$, bearing $\theta_{n,m}$, length $l_{n,m}$, and width $w_{n,m}$ of the detected ships.

Algorithms of both types have been developed and evaluated [49], [50], and several limitations have been noted. First, the fusion of heterogeneous information sources is not straightforward. Second, they do not adapt to time-varying model parameters. Third, their complexity usually does not scale well in relevant system parameters, e.g., the number of sensors.

SPA-BASED MULTISENSOR MTT ALGORITHM

An emerging approach to MTT and information fusion—one with flexibility, low complexity, and useful scalability—is based on a factor graph and the SPA [39], [40], [51]. First, a factor graph representing the statistical model of the MTT problem is derived; then, the SPA is used to obtain a principled and intuitive approximation of the Bayesian inference needed for targets detection and estimation. A major advantage of the SPA is its ability to exploit conditional independence properties of random variables for a drastic reduction of complexity; thereby, SPA-based MTT algorithms can achieve an attractive performance-complexity compromise (see [40] and references therein), making them suitable for large-scale tracking scenarios involving a large number of targets, sensors, and measurements, and allowing their use on resource-limited devices. Generally, the complexity of an SPA-based MTT algorithm scales only quadratically in the number of targets, linearly in the number of sensors, and linearly in the number of measurements per sensor, and outperforms previously proposed methods in terms of accuracy. For the interested reader, simulation results comparing the performance of the SPA-based MTT algorithm with the performance of the (cardinalized) PHD and partition-based (cardinalized) PHD filters are provided in [39] and [51].

The SPA’s versatility and intuitiveness has enabled the establishment of a suite of Bayesian multisensor MTT tracking and information fusion algorithms where, similar to a construction kit system, algorithm parts can be combined, extended, or adapted to achieve desired

**Figure 8.**

Example of factor graph for the case of two targets and two measurements produced by a single sensor at a given time. In addition, the previous, predicted, and current beliefs for the two targets are shown.

functionalities and properties. SPA-based MTT algorithms can be extended to fuse heterogeneous data, e.g., terrestrial radars, SAR, optical sensors, and AIS. They can incorporate different DMs such as nearly constant velocity (NCV) or OU. They can also be designed to infer time-varying model parameters, such as detection probabilities of radar sensors; and to select an index from a menu of multiple target motion models. The use of SPA-based MTT algorithm is promising due to the highly efficient solution of the MOU problem combined with sequential Monte Carlo techniques, and is potentially suitable for arbitrary nonlinear and non-Gaussian problems. The SPA-based MTT algorithm estimates the number of targets K_n and their state at each time n by efficiently solving the MOU problem and calculating the beliefs $\tilde{f}(x_{n,k})$, which approximates the marginal posterior pdfs $f(x_{n,k}|z)$, by employing an iterative version of the SPA on a suitably devised factor graph [39], [40].

The SPA approach is illustrated in Figure 8 via a simple two-target example with two measurements and a single sensor. It is structured into four sections that refer to various beliefs and/or operations within the SPA-based MTT algorithm. The *previous belief* for target $k \in \{1, 2\}$ approximates the marginal posterior pdf of the previous state $x_{n-1,k}$, i.e., $f(x_{n-1,k}|z^-)$, which is represented by the factor node “ f_k^- ” in Figure 8, and where z^- denotes all the measurements up to time $n-1$. In the *prediction* step, the previous belief is converted into the *predicted belief*, which approximates the pdf $f(x_{n,k}|z^-)$. The prediction is performed by utilizing an appropriate DM $f(x_{n,k}|x_{n-1,k})$, which is represented by the factor node “ f_k .” When the time interval between two consecutive time steps is large, e.g., in the order of hours, as for the case of two consecutive SAR images, the OU DM can be used to reduce the prediction uncertainty. In the *measurement update and data association* step, the measurements $z_{n,1}^{(1)}$ and $z_{n,2}^{(1)}$ are used to evaluate the likelihoods $f(z_{n,m}^{(1)}|x_{n,k})$ and solve the MOU problem, as described in [40]. This results in the *current belief*, which approximates the current marginal posterior pdf $f(x_{n,k}|z)$ at time step n . The current belief is centered around the current measurement, and it is used for target detection and for state estimation at the current time step n . In addition to the factor graph, Figure 8

also visualizes the previous, predicted, and current beliefs for the first and second target in the upper and lower three-dimensional plots, respectively. The arrows in the left-hand plots represent the trajectories of the targets. Because of the uncertainty of target-measurement association and the proximity of the two targets, the current beliefs are bimodal. The smaller of the two modes is centered roughly at the position of the respective other target.

MULTIPLE DYNAMIC MODELS AND INTEGRATION OF CONTEXTUAL INFORMATION

Many tracking scenarios, such as those involving maneuvering targets, require the use of different DMs in different time periods in order to better describe targets that maneuver, e.g., alternating between NCV and constant turn-rate motion models. Therefore, following an interacting multiple model approach [52, Ch. 11], the evolution of the state of a target can be modeled by means of a set of possible DMs. A DM index $\ell_{n,k}$ is introduced for each target k to select the most appropriate DM at time n [53], [54]. The DM indices $\ell_{n,k}$ are modeled as discrete random variables that are independent across targets and evolve in time according to a Markov chain. Bayesian inference on the DM indices $\ell_{n,k}$ and the target states $x_{n,k}$ can still be performed by running the SPA algorithm on a suitable devised factor graph.

The multiple DM formalism also permits integration of available contextual information, e.g., geographical constraints, maritime routes, or even MTGs (cf. “AIS-Based Maritime Traffic Knowledge Discovery”), which is not related directly to kinematic sensor measurements. For example, as shown in [16, Ch. 12, 13, 16], this contextual knowledge can often be modeled in a statistical way, and integrated in tracking filters to improve the tracking performance. In particular, considering the case of MTGs, each navigational leg of an MTG, i.e., an edge (i, j) connecting waypoint i to waypoint j , can be associated to a specific dynamic model characterized by a dominant direction, that is, from waypoint i to waypoint j . Still, a discrete random variable $\ell_{n,k}$ can be introduced to select the DM, that is the maritime route, that the target is

following at time n [55]. The evolution of $\ell_{n,k}$ is again modeled by a Markov chain. This results in a multisensor MTT algorithm that automatically takes into account the knowledge of standard maritime routes.

FUSION OF SAT-AIS INFORMATION

The SPA-based MTT algorithm can also be extended to fuse information coming from a Sat-AIS system [55], [56]. The fusion of this information is often difficult due to the asynchronicity and sparsity of the Sat-AIS messages, and the nontrivial association between messages and targets. Indeed, although each Sat-AIS message usually includes a unique maritime mobile service identity (MMSI), this may be absent, or mistaken for a different MMSI, or observed for the first time, in which case no prior information is available on the target-message association. The SPA-based MTT method can be efficiently extended to fuse Sat-AIS messages and measurements obtained from SAR, optical images, or other sensors, and to identify (or label) each detected ship by means of the MMSI. The label associated to each target is modeled as a discrete random variable: marginal posterior pdfs of the targets states $x_{n,k}$ and of the labels can still be efficiently obtained by running the SPA algorithm on a factor graph derived by the underlying statistical formulation of the problem.

CLASSIFICATION-AIDED SPA-BASED MULTITARGET TRACKING

As explained in the section “DNN Architectures for Satellite Image Segmentation and Target Classification,” modern deep learning segmentation and classification techniques are able to provide, in addition to kinematic data, class information for detected ships in satellite images. This information assigns each ship to one category among a predefined finite set of categories, e.g., cargo, dredging-military-sailboat, fishing, high-speed craft, other-unknown-reserved, passenger or pilot boat. The SPA-based MTT approach can be efficiently extended for the exploitation of imperfect *class* information. This class information allows, for instance, the use of class-dependent DMs or measurement models. As a consequence, the inclusion of class information greatly improves the performance of the SPA-based MTT algorithm [57], [58].

USE CASE SCENARIO: SPA-BASED MTT TO FUSE AIS DATA AND SAR MEASUREMENTS

The use-case scenario described in the current section aims at demonstrating how SPA-based MTT methods can be used to fuse measurements (ship detections) extracted from SAR images, which do not provide any information regarding ship identities, and the information contained in the AIS messages, i.e., ship’s position and the MMSI identifier [55], [56].

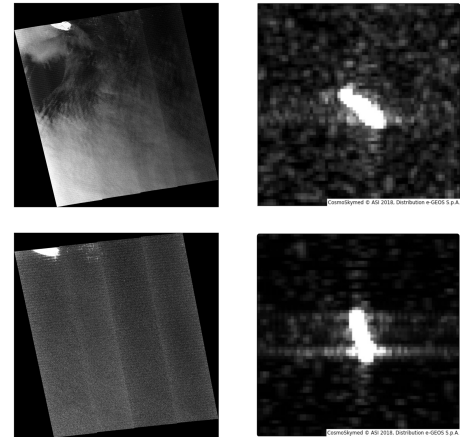
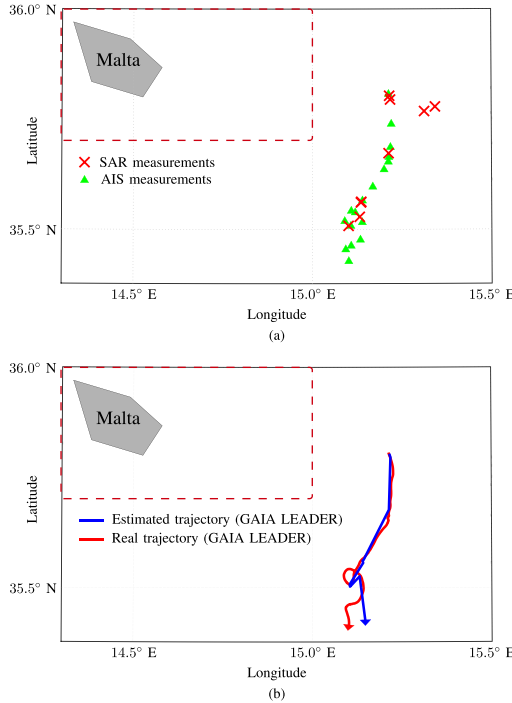


Figure 9.

(Left images) Subsampled (5 times) quicklook SAR images acquired on 9 September 2018 at 04:37 (Left-Top) and on 10 September 2018 at 04:55 (Left-Bottom) by the COSMO-SkyMed constellation. (Right Images) Full resolution SAR images showing detected ships on 9 September 2018 at 04:37 (Top-Right) and on 10 September 2018 at 04:55 (Bottom-Right). (All images are of ASI property and processed by E-GEOS.)

The AIS messages and SAR measurements were collected from an area of the Mediterranean Sea, off the shore of Malta, in the period from 8 September 2018 at 16:30 through 12 September 2018 at 16:47. The SAR measurements are extracted from a sequence of SAR images acquired by the COSMO-SkyMed constellation, by means of AI segmentation techniques as described in “DNN Architectures for Satellite Image Segmentation and Target Classification” and consist of estimated GPS coordinates of the detected targets, i.e., latitude and longitude. The time interval between two consecutive AIS messages is at least of 5 h. Figure 9 shows two examples of subsampled quicklook SAR images (left column) acquired by the COSMO-SkyMed constellation, and two examples of full resolution SAR images (right column) showing detected ships. Due to the MOU problem, it is not known in advance whether a SAR measurement is originated from a target or is a false alarm, and, in the case it has been originated by a target, it is not known by which target.

The main purpose of this use case is, therefore, to fuse SAR measurements with AIS messages in order to track potential targets and also identify them by exploiting the MMSI identifiers. The SAR measurements and AIS messages used by the SPA-based MTT method are represented in Figure 10(a) by the red crosses and green triangles, respectively. The red dashed rectangle delimits a geographical area of little interest from a tracking point of view with a large number of docked ships. Therefore, the SAR measurements and AIS messages from ships within this red dashed rectangle are discarded. The dynamic model used to describe ship motion in the SPA-based MTT algorithm is the OU model. This choice is motivated by the higher accuracy of the OU model in predicting future positions of vessels over a long time horizon (e.g., in the order of hours) compared to a NCV model. Estimated positions of detected

**Figure 10.**

(a) SAR (red crosses) and AIS (green triangles) measurements used by the SPA-based fusion algorithm obtained in the period from 8 September 2018 at 16:30 through 12 September 2018 at 16:47. The measurements inside the red dashed rectangle have not been considered. (b) Estimated and real (derived by AIS messages) trajectories for the vehicles carrier GAIA LEADER obtained using the SAR and AIS measurements.

targets are calculated each time a SAR measurement is obtained, using all AIS messages gathered in the time interval between the current and the previous SAR measurements. Besides estimating the number of targets and their positions, the algorithm associates, when possible, an MMSI identifier to each of them. These MMSI identifiers are selected from a set consisting of all the MMSI identifiers so far observed. Figure 10(b) shows the output of the SPA-based MTT algorithm. One can observe that in the considered time period and area only a single target is present, identified by the algorithm as the vehicles carrier GAIA LEADER; in particular, the red and blue lines represent its real (derived by AIS messages) and estimated trajectories, respectively. The SPA-based MTT algorithm is, therefore, able to provide fused trajectories of the targets using both SAR measurements and AIS messages and allows the identification of each estimated trajectory by associating it to the most likely MMSI identifier.

CONCLUSIONS

The increasing availability of multiple space-based sensors providing detailed images of the ships at the sea calls for the development of advanced image analysis techniques for target detection, segmentation, and classification.

In a companion paper [1], we discussed several satellite sensing technologies for MS. In this article, we reported some of the most recent deep-learning techniques and described their effectiveness in several use cases exploiting SAR, HR, and VHR images. We have presented Bayesian and allied statistical techniques to extract information (for example, common sea-lanes) from repositories of historical Sat-AIS data, and have shown how to track multiple targets using heterogeneous space-based and terrestrial sensors. MTT approaches based on the SPA have gained strong popularity, thanks to their flexibility and scalability. A use case scenario, that described the fusion of measurements extracted from SAR images acquired near the shores of Malta island with Sat-AIS messages, demonstrated the effectiveness of the SPA-based MTT methods in the context of MS using space-based sensors.

ACKNOWLEDGMENTS

This work was supported in part by the NATO Allied Command Transformation under Project SAC000A08. The work of P. Willett was supported in part by NIUVT, and by AFOSR under Grant FA9500-18-1-0463.

REFERENCES

- [1] G. Soldi *et al.*, “Space-based global maritime surveillance Part I: Satellite technologies,” *IEEE Aerosp. Electron. Syst. Mag.*, this issue.
- [2] O. Ronneberger, P. Fischer, and T. Brox, “U-Net: Convolutional networks for biomedical image segmentation,” in *Proc. Med. Image Comput. Comput.-Assist. Intervention*, 2015, vol. 9351, pp. 234–241.
- [3] K. He, X. Zhang, S. Ren, and J. Sun, “Deep residual learning for image recognition,” in *Proc. IEEE Conf. Comput. Vis. Pattern Recognit.*, 2016, pp. 770–778.
- [4] K. He, G. Gkioxari, P. Dollár, and R. Girshick, “Mask R-CNN,” in *Proc. IEEE Int. Conf. Comput. Vis.*, 2017, pp. 2980–2988.
- [5] E. H. Adelson, C. H. Anderson, J. R. Bergen, P. J. Burt, and J. M. Ogden, “Pyramid methods in image processing,” *RCA Eng.*, vol. 29, no. 6, pp. 33–41, 1984.
- [6] N. A. Bomberger, B. J. Rhodes, M. Seibert, and A. M. Waxman, “Associative learning of vessel motion patterns for maritime situation awareness,” in *Proc. 9th Int. Conf. Inf. Fusion*, 2006, pp. 1–8.
- [7] B. J. Rhodes, N. A. Bomberger, and M. Zandipour, “Probabilistic associative learning of vessel motion patterns at multiple spatial scales for maritime situation awareness,” in *Proc. 10th Int. Conf. Inf. Fusion*, 2007, pp. 1–8.
- [8] B. Ristic, B. La Scala, M. Morelande, and N. Gordon, “Statistical analysis of motion patterns in AIS data: Anomaly detection and motion prediction,” in *Proc. 11th Int. Conf. Inf. Fusion*, 2008, pp. 1–7.

- [9] G. Pallotta, M. Vespe, and K. Bryan, "Vessel pattern knowledge discovery from AIS data: A framework for anomaly detection and route prediction," *Entropy*, vol. 15, no. 6, pp. 2218–2245, 2013.
- [10] Z. Xiao, L. Ponnambalam, X. Fu, and W. Zhang, "Maritime traffic probabilistic forecasting based on vessels' waterway patterns and motion behaviors," *IEEE Trans. Intell. Transp. Syst.*, vol. 18, no. 11, pp. 3122–3134, Nov. 2017.
- [11] P. Coscia, P. Braca, L. M. Millefiori, F. A. N. Palmieri, and P. Willett, "Multiple Ornstein-Uhlenbeck processes for maritime traffic graph representation," *IEEE Trans. Aerosp. Electron. Syst.*, vol. 54, no. 5, pp. 2158–2170, Oct. 2018.
- [12] N. Forti, L. Millefiori, and P. Braca, "Unsupervised extraction of maritime patterns of life from automatic identification system data," in *Proc. OCEANS Marseille*, 2019, pp. 1–5.
- [13] R. Falcon, R. Abielmona, and E. Blasch, "Behavioral learning of vessel types with fuzzy-rough decision trees," in *Proc. 17th Int. Conf. Inf. Fusion*, 2014, pp. 1–8.
- [14] M. Guerrero, P. Willett, S. Coraluppi, and C. Carthel, "Radar/AIS data fusion and SAR tasking for maritime surveillance," in *Proc. 11th Int. Conf. Inf. Fusion*, 2008, pp. 1–5.
- [15] G. Pallotta and A. Jousselme, "Data-driven detection and context-based classification of maritime anomalies," in *Proc. 18th Int. Conf. Inf. Fusion*, 2015, pp. 1152–1159.
- [16] L. Snidaro, J. García, J. Llinas, and E. Blasch, *Context-Enhanced Information Fusion*. Cham, Switzerland: Springer, 2016.
- [17] L. M. Millefiori, P. Braca, K. Bryan, and P. Willett, "Modeling vessel kinematics using a stochastic mean-reverting process for long-term prediction," *IEEE Trans. Aerosp. Electron. Syst.*, vol. 52, no. 5, pp. 2313–2330, Oct. 2016.
- [18] Z. Xiao, X. Fu, L. Zhang, and R. S. M. Goh, "Traffic pattern mining and forecasting technologies in maritime traffic service networks: A comprehensive survey," *IEEE Trans. Intell. Transp. Syst.*, vol. 21, no. 5, pp. 1796–1825, May 2020.
- [19] D. Zisis, K. Chatzikokolakis, G. Spiliopoulos, and M. Vodas, "A distributed spatial method for modeling maritime routes," *IEEE Access*, vol. 8, pp. 47 556–47 568, 2020.
- [20] A. Valsamis, K. Tserpes, D. Zisis, D. Anagnostopoulos, and T. Varvarigou, "Employing traditional machine learning algorithms for big data streams analysis: The case of object trajectory prediction," *J. Syst. Softw.*, vol. 127, pp. 249–257, 2017.
- [21] D. Nguyen, R. Vadaine, G. Hajduch, R. Garello, and R. Fablet, "A multi-task deep learning architecture for maritime surveillance using AIS data streams," in *Proc. IEEE Int. Conf. Data Sci. Adv. Analytics*, 2018, pp. 331–340.
- [22] N. Forti, L. M. Millefiori, P. Braca, and P. Willett, "Prediction of vessel trajectories from AIS data via sequence-to-sequence recurrent neural networks," in *Proc. IEEE Int. Conf. Acoust., Speech, Signal Process.*, 2020, pp. 8936–8940.
- [23] L. Cazzanti, A. Davoli, and L. M. Millefiori, "Automated port traffic statistics: From raw data to visualisation," in *Proc. IEEE Int. Conf. Big Data*, 2016, pp. 1569–1573.
- [24] Y. Li, R. W. Liu, J. Liu, Y. Huang, B. Hu, and K. Wang, "Trajectory compression-guided visualization of spatio-temporal AIS vessel density," in *Proc. 8th Int. Conf. Wireless Commun. Signal Process.*, 2016.
- [25] L. M. Millefiori, P. Braca, and P. Willett, "Consistent estimation of randomly sampled Ornstein-Uhlenbeck process long-run mean for long-term target state prediction," *IEEE Signal Process. Lett.*, vol. 23, no. 11, pp. 1562–1566, Nov. 2016.
- [26] L. M. Millefiori, G. Pallotta, P. Braca, S. Horn, and K. Bryan, "Validation of the Ornstein-Uhlenbeck route propagation model in the mediterranean sea," in *Proc. OCEANS*, 2015, pp. 1–6.
- [27] L. M. Millefiori, P. Braca, and G. Arcieri, "Scalable distributed change detection and its application to maritime traffic," in *Proc. IEEE Int. Conf. Big Data*, 2017, pp. 1650–1657.
- [28] M. Ester, H.-P. Kriegel, J. Sander, and X. Xu, "A density-based algorithm for discovering clusters in large spatial databases with noise," in *Proc. Int. Conf. Data Mining Knowl. Discov.*, 1996, vol. 4, pp. 226–231.
- [29] R. O. Lane, D. A. Nevell, S. D. Hayward, and T. W. Beane, "Maritime anomaly detection and threat assessment," in *Proc. 13th Int. Conf. Inf. Fusion*, 2010, pp. 1–8.
- [30] K. Kowalska and L. Peel, "Maritime anomaly detection using Gaussian process active learning," in *Proc. 15th Int. Conf. Inf. Fusion*, 2012, pp. 1164–1171.
- [31] M. Vespe, I. Visentini, K. Bryan, and P. Braca, "Unsupervised learning of maritime traffic patterns for anomaly detection," in *Proc. 9th IET Data Fusion Target Tracking Conf.*, 2012, pp. 1–5.
- [32] E. d'Afflisio, P. Braca, L. M. Millefiori, and P. Willett, "Detecting anomalous deviations from standard maritime routes using the Ornstein-Uhlenbeck process," *IEEE Signal Process. Lett.*, vol. 66, no. 24, pp. 6474–6487, Dec. 2018.
- [33] E. d'Afflisio, P. Braca, L. M. Millefiori, and P. Willett, "Maritime anomaly detection based on mean-reverting stochastic processes applied to a real-world scenario," in *Proc. 21st Int. Conf. Inf. Fusion*, 2018, pp. 1171–1177.
- [34] N. Forti, L. M. Millefiori, and P. Braca, "Hybrid Bernoulli filtering for detection and tracking of anomalous path deviations," in *Proc. 21st Int. Conf. Inf. Fusion*, 2018, pp. 1178–1184.
- [35] N. Forti, L. M. Millefiori, P. Braca, and P. Willett, "Anomaly detection and tracking based on mean-reverting processes with unknown parameters," in *Proc. IEEE Int. Conf. Acoust., Speech Signal Process.*, 2019, pp. 8449–8453.
- [36] N. Forti, L. M. Millefiori, P. Braca, and P. Willett, "Random finite set tracking for anomaly detection in the presence of clutter," in *Proc. IEEE Radar Conf.*, 2020, pp. 1–6.

- [37] N. Forti, G. Battistelli, L. Chisci, and B. Sinopoli, "Joint attack detection and secure state estimation of cyber-physical systems," *Int. J. Robust Nonlinear Control*, 2019.
- [38] G. Vivone, P. Braca, and J. Horstmann, "Knowledge-based multitarget ship tracking for HF surface wave radar systems," *IEEE Trans. Geosci. Remote Sens.*, vol. 53, no. 7, pp. 3931–3949, Jul. 2015.
- [39] F. Meyer, P. Braca, P. Willett, and F. Hlawatsch, "A scalable algorithm for tracking an unknown number of targets using multiple sensors," *IEEE Trans. Signal Process.*, vol. 65, no. 13, pp. 3478–3493, Jul. 2017.
- [40] F. Meyer *et al.*, "Message passing algorithms for scalable multitarget tracking," *Proc. IEEE*, vol. 106, no. 2, pp. 221–259, Feb. 2018.
- [41] Y. Bar-Shalom, P. K. Willett, and X. Tian, *Tracking and Data Fusion: A Handbook of Algorithms*. Storrs, CT, USA: Yaakov Bar-Shalom, 2011.
- [42] D. B. Reid, "An algorithm for tracking multiple targets," *IEEE Trans. Autom. Control*, vol. 24, no. 6, pp. 843–854, Dec. 1979.
- [43] C. Chong, S. Mori, and D. B. Reid, "Forty years of multiple hypothesis tracking—A review of key developments," in *Proc. 21st Int. Conf. Inf. Fusion*, 2018, pp. 452–459.
- [44] R. Mahler, *Statistical Multisource-Multitarget Information Fusion*. Norwood, MA, USA: Artech House, 2007.
- [45] R. P. S. Mahler, "Multitarget Bayes filtering via first-order multitarget moments," *IEEE Trans. Aerosp. Electron. Syst.*, vol. 39, no. 4, pp. 1152–1178, Oct. 2003.
- [46] R. Mahler, "PHD filters of higher order in target number," *IEEE Trans. Aerosp. Electron. Syst.*, vol. 43, no. 4, pp. 1523–1543, Oct. 2007.
- [47] B.-T. Vo, B.-N. Vo, and A. Cantoni, "Analytic implementations of the cardinalized probability hypothesis density filter," *IEEE Trans. Signal Process.*, vol. 55, no. 7, pp. 3553–3567, Jul. 2007.
- [48] B.-T. Vo, B.-N. Vo, and A. Cantoni, "The cardinality balanced multi-target multi-Bernoulli filter and its implementations," *IEEE Trans. Signal Process.*, vol. 57, no. 2, pp. 409–423, Feb. 2009.
- [49] A. M. Ponsford and J. Wang, "A review of high frequency surface wave radar for detection and tracking of ships," *Turkish J. Electron. Eng. Comput. Sci.*, vol. 18, pp. 409–428, May 2010.
- [50] S. Maresca, P. Braca, J. Horstmann, and R. Grasso, "Maritime surveillance using multiple high-frequency surface-wave radars," *IEEE Trans. Geosci. Remote Sens.*, vol. 52, no. 8, pp. 5056–5071, Aug. 2014.
- [51] D. Gaglione *et al.*, "Bayesian information fusion and multitarget tracking for maritime situational awareness," *IET Radar Sonar Navigation*, vol. 14, pp. 1845–1857, Dec. 2020.
- [52] Y. Bar-Shalom, X. R. Li, and T. Kirubarajan, *Estimation With Applications to Tracking and Navigation*. New York, NY, USA: Wiley, 2001.
- [53] G. Soldi and P. Braca, "Online estimation of unknown parameters in multisensor-multitarget tracking: A belief propagation approach," in *Proc. 21st Int. Conf. Inf. Fusion*, 2018, pp. 2151–2157.
- [54] G. Soldi, F. Meyer, P. Braca, and F. Hlawatsch, "Self-tuning algorithms for multisensor-multitarget tracking using belief propagation," *IEEE Trans. Signal Process.*, vol. 67, no. 15, pp. 3922–3937, Aug. 2019.
- [55] G. Soldi *et al.*, "Heterogeneous information fusion for multitarget tracking using the sum-product algorithm," in *Proc. IEEE Int. Conf. Acoust., Speech, Signal Process.*, 2019, pp. 5471–5475.
- [56] D. Gaglione, P. Braca, and G. Soldi, "Belief propagation based AIS/radar data fusion for multi-target tracking," in *Proc. Int. Conf. Inf. Fusion*, 2018, pp. 2143–2150.
- [57] D. Gaglione, G. Soldi, P. Braca, G. De Magistris, F. Meyer, and F. Hlawatsch, "Classification-aided multitarget tracking using the sum-product algorithm," *IEEE Signal Process. Lett.*, vol. 27, pp. 1710–1714, 2020.
- [58] G. Soldi *et al.*, "Underwater tracking based on the sum-product algorithm enhanced by a neural network detections classifier," in *Proc. IEEE Int. Conf. Acoust., Speech, Signal Process.*, 2020, pp. 5460–5464.